Downloaded 08/28/21 to 69.181.137.94. Redistribution subject to SEG license or copyright; see Terms of Use at http://library.seg.org/page/policies/terms
DOI:10.1190/segam2020-3418917.1

The Wolfspar® experience: Learnings from processing sparse, low-frequency seismic data

Andrew Brenders, Joe Dellinger, Imtiaz Ahmed, Esteban Díaz, Mariana Gherasim, Hu Jin, and Madhav Vyas, BP America Inc.*

Summary

A 3-D field trial of *Wolfspar*, a low-frequency marine seismic source ("LFS") developed by BP, was conducted over the Mad Dog field in the US Gulf of Mexico in 2018. LFS data were shot on a very coarse grid (280 m inline, 2 to 4 km crossline) and recorded into a spread of Ocean-Bottom Nodes (OBN) simultaneously with airgun sources shooting on a conventional dense grid (50 m inline, 50 m crossline sampling). Analysis of the recorded low-frequency data from both the LFS and conventional airguns showed a significant improvement in signal-to-noise (S/N) quality over the design frequency range of 1.7 to 2.5 Hz, especially at long offsets. However, using the LFS data with FWI to improve the velocity model for imaging produced only an incremental uplift in the sub-salt image quality in the reservoir zone, albeit with clear improvements at depths of greater than 25,000 feet.

To better understand these results we re-examined the data, the processing, and the FWI model updates. We found that (1) the LFS achieved its design S/N goals over its frequency range; (2) the wave-extrapolation and imaging operators built into FWI and migration are very effective at suppressing low-frequency noise, so that densely sampled data even with a very low S/N (such as from airguns) can still produce useable model updates; (3) data density becomes less important at wider offsets. The results of this study have implications for future acquisition designs with low-frequency seismic sources going forward.

Introduction

In 2003-2004, one of the widely accepted barriers to successful full-waveform inversion (FWI) was the requirement that seismic data possess both low frequencies and long offsets, neither of which were commonly recorded by standard seismic acquisition designs of the early 2000's. This understanding, combined with synthetic imaging experiments using finite-difference modelling, helped support investments in several novel acquisition technologies including Wide-Azimuth Towed Streamers (WAZ / WATS) and Ocean Bottom Nodes (OBN). These technologies were focused on the receiver side of the problem and were initially tested at two fields already under development in the Gulf of Mexico: WATS at Mad Dog in 2004, and OBN at Atlantis in 2005. On the source side, several low-frequency design concepts were initiated by various seismic contractors and resource companies, including *Wolfspar* (Dellinger et al., 2016).

Contemporaneously to the development and field testing of new seismic acquisition concepts a computationally efficient version of 3-D FWI was developed at BP, enabling the first production-scale tests in late 2005-2006 (Sirgue et al., 2010). One of the primary targets for 3-D FWI was the Atlantis field in the Gulf of Mexico, which suffered from severe sub-salt illumination and velocity model problems. Although the 2005 OBN survey mitigated some of the illumination issues, the data, even with full-azimuth and long-offset acquisition, did not improve the velocity model enough to solve all the underlying imaging issues. Synthetic tests with FWI, however, suggested that if we could start the process with data including temporal frequencies of approximately 1.4 Hz, large-scale sub-salt velocity errors could be corrected by FWI (Dellinger et al., 2017).

A 4-D monitor survey was acquired at Atlantis in 2015 with an expanded acquisition specifically designed to better record lower frequencies and longer offsets for improved FWI (van Gestel et al., 2015). Figure 1 shows the phase at 2.25 Hz of common-receiver-gathers from the 2005 and 2015 surveys, extracted via Fourier transform. Note the clear improvement in S/N at long offsets in 2015 versus 2005, and the larger maximum offsets recorded in 2015 versus 2005 (nearly double). As hoped, the better data, coupled with improved FWI workflows and algorithms, produced a dramatically improved velocity model and sub-salt image (Shen et al., 2017, 2018).

If improved S/N at even lower frequencies and longer offsets could be recorded, shouldn't we obtain a better FWI result? In late 2017 - early 2018 we performed this experiment at Mad Dog using *Wolfspar*, a novel source optimized to produce low frequencies, augmenting an airgun survey using a 5110 cu. in. array (Pool et al., 2018). Although the new source achieved excellent S/N levels at frequencies as low as 1.68 Hz, exactly as it was designed to do, the inclusion of the LFS data in the FWI produced only a modest uplift in the final image relative to FWI with the airgun data alone (Brenders et al., 2018). To understand why the resulting velocity models were so similar despite the clearly superior S/N of the LFS data, we performed an analysis to investigate how FWI works on the two different types of data, which had very different acquisition geometries.

Survey design for low-frequency seismic acquisition

At Mad Dog, source lines were acquired with two different operating "sweep profiles," to test two different strategies for using the device. Profile 1 was designed to go as low in

© 2020 Society of Exploration Geophysicists

10.1190/segam2020-3418917.1

Downloaded 08/28/21 to 69.181.137.94. Redistribution subject to SEG license or copyright; see Terms of Use at http://library.seg.org/page/policies/terms
DOI:10.1190/segam2020-3418917.1

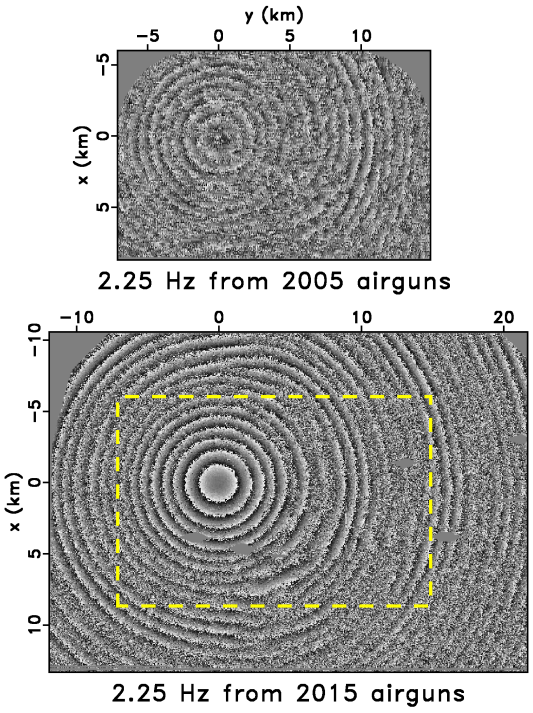


Figure 1. Common-receiver-gathers (CRG) showing the phase of 2.25 Hz data from the 2005 (top) and 2015 (bottom) Atlantis OBN surveys plotted at the same map scale. The airgun source is located at the center of the bullseye pattern, at coordinate (0,0). The dashed box shows the relative extent of a 2005 CRG versus a 2015 CRG.

frequency as possible while still producing excellent S/N. As designed, profile 1 produced data over the range of 1.7 - 2.5 Hz with near-synthetic S/N out to offsets of 30 km (Dellinger et al., 2019). For profile 1 the source was towed at a depth of 60 m. The lower resonating limit of the source is determined by the tow depth: the shallower the operating depth, the lower the frequencies that can be reached. Profile 2 was designed to operate near the lowest usable frequency limit of the device. For profile 2 the LFS was towed at a depth of 36 m, producing data over the range 1.45 – 2.0 Hz. Model studies suggested the S/N for this shallower operating profile would be significantly lower than for profile 1, but still adequate for FWI.

The *Wolfspar* field trial was a "survey of opportunity," taking advantage of an existing airgun survey pre-designed with a rolling patch of OBNs. The plan was to execute the field trial within a span of time when nearly the entire node patch would be deployed. To cover the entire sourcing area in a little more than a week of operations, shot lines were coarsely spaced, in most cases 4 km apart (see Figure 2). We judged this to be sufficient for a time- and cost-limited "proof of concept" survey.

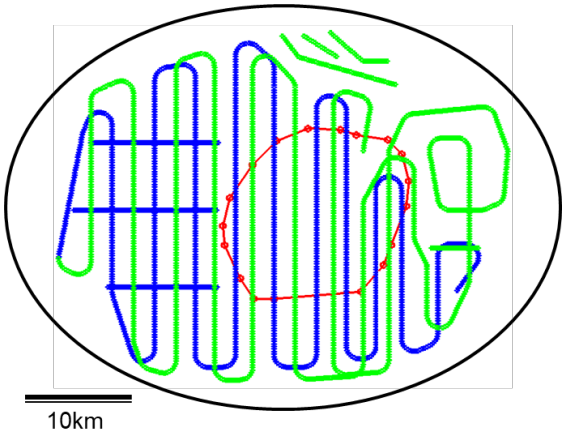


Figure 2. Designed *Wolfspar* acquisition geometry during the Mad Dog field trial. Red – OBN patch outline; Green – shot lines for sweep profile 1; Blue – shot lines for sweep profile 2. Shot lines for the same source signatures average about 4 km apart.

The quality of quantity

Airguns at Mad Dog were shot on a 50 x 50 m grid over 3 months of acquisition. Even though there were several hundred airgun shots per LFS shot point (approx. 280 m inline spacing), calculations showed that the 1.7 – 2.5 Hz LFS shot lines, as a whole, should still impart several times more low-frequency acoustic power per unit area into the Earth over this frequency range than the complete airgun survey. Analysis of common-shot and common-receiver gathers from the field trial supported this.

Figure 3 compares the phase of Mad Dog data for multiple, stacked airgun and *Wolfspar* shots for frequencies between 1.40 and 1.80 Hz. The location of the LFS shot and the airgun shots was approximately equivalent. Each shot was recorded into the entire array of ~2000 OBN. The top and middle panels of Figure 3 show stacks of the nearest 25 and 100 airgun shots, respectively, surrounding the LFS shot point (bottom panel). Figure 4 illustrates how the airgun shot points in Figure 3 were chosen for stacking. As expected, a common-shot gather from the LFS produced excellent S/N at 1.7 Hz, better than either 25 or 100 airgun shots stacked together. However, note that since the broadband amplitude spectrum of airgun sources continues to smoothly taper off for lower frequencies, unlike for the LFS, some coherent signal below 1.7 Hz can still be observed in the airgun data, albeit with a rapid reduction in S/N as a function of offset.

Plessix (2010) notes that FWI often seems to work even for frequencies where no coherent phase is evident in the raw data. At the frequencies of interest in this survey (< 2.5 Hz), the airgun S/N is lower, but is it still good enough for FWI?

© 2020 Society of Exploration Geophysicists

10.1190/segam2020-3418917.1

Downloaded 08/28/21 to 69.181.137.94. Redistribution subject to SEG license or copyright; see Terms of Use at http://library.seg.org/page/policies/terms
DOI:10.1190/segam2020-3418917.1

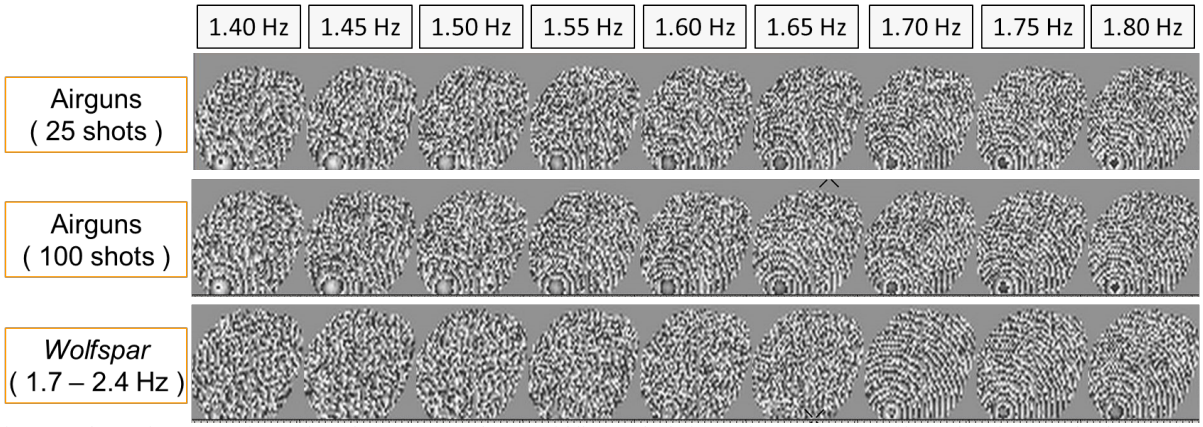


Figure 3: Phase of common-shot gathers for 25 (top) and 100 (middle) stacked airgun shots and one *Wolfspar* shot (bottom) for frequencies from 1.4 to 1.8 Hz. The shot location is the "bullseye" in the bottom left corner of the node patch. The maximum offsets, at the top right of the node patch, are about 18km. The S/N benefits of stacking the airguns are clearly visible. The lowest frequency in the sweep is about 1.68 Hz, so no signal is visible for the frequency panels at 1.65 Hz and below. At 1.70 Hz and above, a single LFS shot produces significantly better S/N than 100 stacked airguns. This difference is especially notable at the widest offsets.

When evaluating the impact of S/N on FWI with low-frequency seismic data from different seismic sources and different acquisition geometries, compute cost is a concern, as the iterative nature of FWI can become cost prohibitive for 3-D scenario testing. Instead, we used the relationship between FWI and reverse-time migration (RTM) to make some approximations. The RTM imaging condition can be written as

$$I(x,y,z,\,\omega) = \int \sum_{s} \sum_{r} \psi_s(x,y,z,\omega)\psi^*_{r(s)}\,(x,y,z,\omega)d\omega$$

while the FWI gradient can be written

$$\delta v(x,y,z,\,\omega) = \alpha \int \sum_{s} \sum_{r} \omega^2 \psi_s(x,y,z,\omega)\delta\psi^*_{r(s)}\,(x,y,z,\omega)d\omega$$

where ω is angular frequency, ψ_s is the source wavefield, ψ_s is the receiver wavefield, $\delta\psi^*_{r(s)}$ is the receiver residual wavefield, I is the RTM image, and δv is the FWI model update. Since the first iteration of FWI is approximately equal to an iteration of RTM, we can get a good idea of how FWI will use low-frequency data by first migrating the data, followed by an evaluation and comparison of the resulting low-frequency image with the gradient from the first iteration of FWI.

Figure 5 shows some of the 3-D, frequency-domain, single-frequency RTM images computed using low-frequency data from *Wolfspar* (Figure 5a) and airguns (Figure 5b-d). The section displayed is located at a near-zero crossline offset from an LFS shot line, with the next closest crossline 2 km away. When comparing a low-frequency airgun migration, to avoid interpretation bias from incidental differences in the acquisition geometry, in Figure 5b we used the nearest 140 airgun shots to each LFS shot point (see Figure 4). The airgun image is not noticeably further improved if additional airgun shots are used. Figures 5a and 5b are of roughly similar quality, despite the 2 - 4 km crossline spacing of the LFS data. The airgun image (5b) contains more noise, but this is comparable to the "ringier" acquisition footprint in the *Wolfspar* image (5a). Figures 5c and 5d demonstrate how the fidelity of the image decreases if fewer low-frequency airgun shots are used. These tests showed that: 1) the quality of the image improves with the number of airgun shots, but only up to a point, and then levels off; 2) the acquisition footprint from the coarse crossline spacing of the LFS data is most noticeable at near offsets.

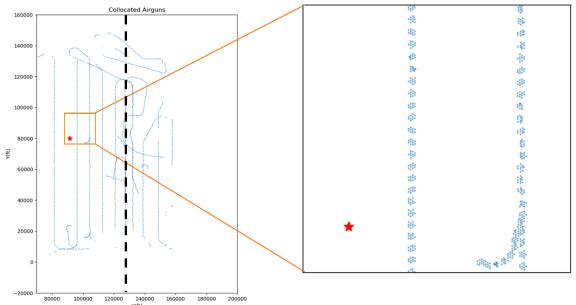


Figure 4: Close-up of selection of "co-located" airgun shots for stacking, analysis, and inclusion in FWI. The left figure shows selected *Wolfspar* shot lines "as shot" for source profile 1, with the 10 closest airgun shots to each LFS shot selected on the right. The red star shows the location of an ocean bottom node. The dashed line shows the location of the migrated section shown in Figure 5, aligned with one of the 2 km infill lines added to the original survey design.

© 2020 Society of Exploration Geophysicists

10.1190/segam2020-3418917.1

Downloaded 08/28/21 to 69.181.137.94. Redistribution subject to SEG license or copyright; see Terms of Use at http://library.seg.org/page/policies/terms
DOI:10.1190/segam2020-3418917.1

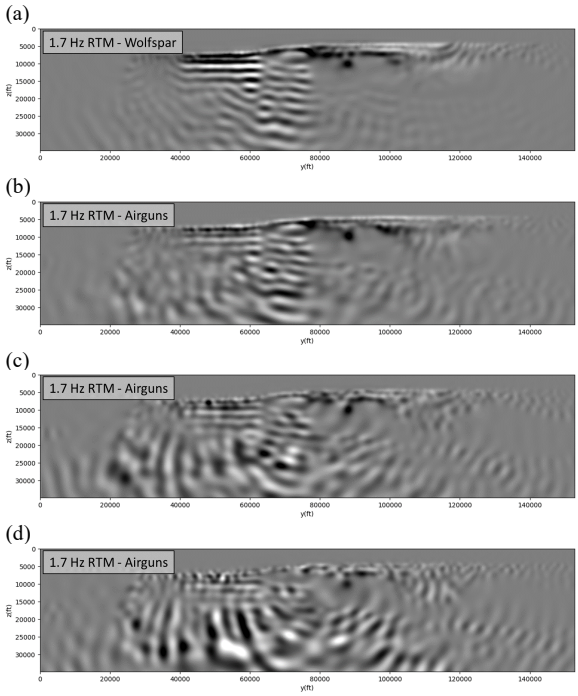


Figure 5: (a) An inline slice from a common-shot domain, mono-frequency RTM image constructed using 1.7 Hz data from *Wolfspar*, shot with a source signature of ~1.7 – 2.5 Hz (profile 1) and an inline spacing of about 280 m. Panels (b-d) show corresponding single-frequency migrations calculated using the nearest airgun shot(s) for each LFS shot point: (b) the nearest 140 airgun shots for each LFS shot; (c) the nearest 10 airgun shots; (d) the nearest 1 airgun shot for each LFS shot.

Discussion

At 1.7 Hz, the far-field power output of *Wolfspar* profile 1 is about 197 dB re $\mu Pa^2/Hz$ @ 1 m, which is about 25 dB higher than the output of the airguns at that frequency (Dellinger et al., 2019). Note that by using power rather than energy we account for the longer repeat interval of the low-frequency source (~120 s), which translates into a coarser inline sampling of our low-frequency source relative to airguns. However, we are not accounting for the denser crossline spacing of airguns: 2 km / 50 m = 40x, adding another 16 dB to the total power output by airguns at low frequencies, which still leaves the LFS with a 9 dB advantage. This is consistent with what we observe in the raw data: at 1.7 Hz the LFS data are significantly better. However, the difference in the migrated images is less obvious, implying that for FWI the low-frequency data from the two very different surveys, with their very different acquisition strategies, was of roughly similar quality.

The lack of significant differences between FWI results with and without the sparse, low-frequency source data can be partially explained by considering the effect of the migration operator on densely sampled airgun sources. In theory, by using an appropriate wavefield extrapolation operator these sources can add coherently, producing up to double the dB advantage to sources adding incoherently (i.e., only adding energy, not amplitude). In addition, we noted that propagation via the wave equation strongly discriminates against energy that cannot be represented as a coherent wave – but only if the sampling is good enough to record the waves coherently. These considerations argue for denser crossline sampling and less emphasis on improving the S/N in raw, unmigrated data. Note that the lower the frequency, the less dense the crossline sampling needed to achieve this coherent stacking effect should be. These findings are consistent with the results of studies examining FWI with wide-offset airgun data (Mei et al., 2019).

Acquiring 20 - 80x the number of shot lines takes time and money, even after accounting for possible savings from multi-boat simultaneous acquisition and wide, multi-source tows on each boat. The cost of acquiring wide offsets and dense shot lines in the same survey are particularly high. Most significantly, we have found that at larger offsets the processing advantage of denser sampling becomes less significant. These considerations suggest that for offsets of 20 km or greater, the concept of a powerful low-frequency source acquired on a coarse shot grid remains attractive for improving the efficiency of seismic acquisition for deep targets. The Mad Dog acquisition acquired nearly all the *Wolfspar* shots into nearly all the nodes in less than two weeks of acquisition. Most airgun shots were acquired into only a subset of the nodes, and this acquisition (which covered the same sourcing area) required months.

Conclusions

The concept of a powerful low-frequency marine source shot on a coarse crossline grid remains viable but appears to be most useful at ultra-wide offsets (20 km+), augmenting a denser acquisition at nearer offsets. Denser acquisition could be with conventional sources like airguns, but it could also include a specialized low-frequency source. With denser acquisition, a low-frequency source could operate at lower frequencies, with correspondingly less S/N, than it could otherwise. Like airguns, a low-frequency source can also take advantage of coherent summation and the powerful S/N-enhancing properties of processing using the wave equation to achieve lower frequencies. Full realization of the potential efficiencies from sparse, low-frequency acquisition may require a step-change in OBN technologies.

Acknowledgements

We would like to thank BP, BHP Petroleum (Deep Water), and Union Oil of California, an affiliate of Chevron USA, Inc., for permission to publish this work.

© 2020 Society of Exploration Geophysicists

REFERENCES

Brenders, A., J. Dellinger, C. Kanu, Q. Li, and S. Michell, 2018, The Wolfspar® field trial: Results from a low-frequency seismic survey designed for FWI: 88th Annual International Meeting, SEG, Expanded Abstracts, 1083–1087, doi: https://doi.org/10.1190/segam2018-2996201.1.

Dellinger, J., A. J. Brenders, R. Pool, C. Kanu, Q. Li, S. Michell, H. Jin, M. Gherasim, S. LaDart, J. R. Sandschaper, E. Díaz, K. Fu, T. Yang, D. Ni, and T. Manning, 2019, The Wolfspar® Field Trial: Testing a new paradigm for low-frequency 3-D velocity surveys: 81st Annual International Conference and Exhibition, EAGE, Extended Abstracts, 1–5, doi: https://doi.org/10.3997/2214-4609.201901273.

Dellinger, J., A. J. Brenders, J. R. Sandschaper, C. Regone, J. Etgen, I. Ahmed, and K. J. Lee, 2017, The Garden Banks model experience: The Leading Edge, **36**, 151–158, doi: https://doi.org/10.1190/tle36020151.1.

Dellinger, J., A. Ross, D. Meaux, A. Brenders, G. Gesoff, J. Etgen, J. Naranjo, G. Openshaw, and M. Harper, 2016, Wolfspar®, an "FWI-friendly" ultralow-frequency marine seismic source: 86th Annual International Meeting, SEG, Expanded Abstracts, 4891–4895, doi: https://doi.org/10.1190/segam2016-13762702.1.

Mei, J., Z. Zhang, F. Lin, R. Huang, P. Wang, and C. Mifflin, 2019, Sparse nodes for velocity: Learnings from Atlantis OBN full-waveform inversion test: 89th Annual International Meeting, SEG, Expanded Abstracts, 167–171, doi: https://doi.org/10.1190/segam2019-3215208.1.

Plessix, R.-E., and C. Perkins, 2010, Full-waveform inversion of a deep water ocean-bottom seismometer dataset: First Break, **28**, 71–78, doi: https://doi.org/10.3997/1365-2397.2010013.

Pool, R., C. Kanu, A. Brenders, and J. Dellinger, 2018, The Wolfspar® Field Trial: Design and execution of a low-frequency seismic survey in the Gulf of Mexico: 88th Annual International Meeting, SEG, Expanded Abstracts, 91–96, doi: https://doi.org/10.1190/segam2018-2997327.1.

Shen, X., I. Ahmed, A. Brenders, J. Dellinger, J. Etgen, and S. Michell, 2017, Salt model building at Atlantis with full-waveform inversion: 87th Annual International Meeting, SEG, Expanded Abstracts, 1507–1511, doi: https://doi.org/10.1190/segam2017-17738630.1.

Shen, X., I. Ahmed, A. Brenders, J. Dellinger, J. Etgen, and S. Michell, 2018, Full-waveform inversion: The next leap forward in subsalt imaging: The Leading Edge, **37**, 67b1–67b6, doi: https://doi.org/10.1190/tle37010067b1.1.

Sirgue, L., O. I. Barkved, J. Dellinger, J. Etgen, U. Albertin, and J. H. Kommedal, 2010, Full waveform inversion: The next leap forward in imaging at Valhall: First Break, **28**, 65–70, doi: https://doi.org/10.3997/1365-2397.2010012.

Van Gestel, J.-P., E. L'Heureux, J. R. Sandschaper, P.-O. Ariston, N. D. Bassett, and S. Dadi, 2015, Atlantis "beyond 4D" ocean bottom nodes acquisition design: 85th Annual International Meeting, SEG, Expanded Abstracts, 125–129, doi: https://doi.org/10.1190/segam2015-5847522.1.

Downloaded 08/28/21 to 69.181.137.94. Redistribution subject to SEG license or copyright; see Terms of Use at http://library.seg.org/page/policies/terms
DOI:10.1190/segam2020-3418917.1